

Establishment and characterization of unique cell lines derived from pyothorax-associated lymphoma which develops in long-standing pyothorax and is strongly associated with Epstein-Barr virus infection

Tetsuya Takakuwa,¹ Wen-Juan Luo,¹ Maria Francisca Ham,¹ Masao Mizuki,² Keiji Iuchi³ and Katsuyuki Aozasa^{1,4}

¹Departments of Pathology and ²Hematology/Oncology, Osaka University Graduate School of Medicine, 2-2 Yamada-oka, Suita, Osaka 565-0871; and ³Department of Surgery, National Kinki-Chuo Hospital, 1180 Nagasone-cho, Sakai, Osaka 591-8025

(Received June 11, 2003/Revised August 6, 2003/Accepted August 7, 2003)

Malignant lymphoma frequently develops in the pleural cavity of patients with over 20 years' history of pyothorax. The term pyothorax-associated lymphoma (PAL) has been proposed for this type of tumor. We established four novel lymphoma cell lines (OPL-3, -4, -5, and -7) from four patients with PAL. Characteristics of the four cell lines are as follows: B-cell nature with defective expression of B-cell and T-cell surface antigens, monoclonal pattern of Epstein-Barr virus (EBV) infection in lymphoma cells (thus indicating an etiological role of EBV for lymphomagenesis), complicated chromosomal abnormalities with numerous structural and numerical abnormalities, and occasional but distinct genome instability. These abnormalities in cell character might be caused by the specific circumstances of PAL lymphomagenesis, i.e., chronic inflammation. Thus, PAL cell lines could be useful in analysis of molecular mechanisms leading to malignancy in chronic inflammation. (Cancer Sci 2003; 94: 858–863)

Malignant lymphoma frequently develops in the pleural cavity of patients with over 20 years' history of pyothorax.¹⁾ The term pyothorax-associated lymphoma (PAL) has been proposed by Aozasa K. for this type of tumor.²⁾ Most PALs are diffuse large cell lymphomas of B-cell type, but unusual types of PAL have also been reported. Al Satti *et al.*³⁾ reported a PAL-derived cell line with dual B- and T-cell phenotype. Daibata *et al.*⁴⁾ reported one cell line of PAL which expressed both CD2 and CD20, but did not express representative B-cell markers or T-cell markers CD1, CD3, CD5, CD7, and CD9.

Replication error (RER) phenotype, as revealed by widespread microsatellite instability (MSI), is a manifestation of genome instability caused by a defect in DNA mismatch repair function, and facilitates the fixation of genetic damage.⁵⁾ MSI has been detected in cancers associated with the hereditary non-polyposis colorectal cancer syndrome, as well as in a variety of sporadic cancers. However, MSI was also reported to have been found in colonic mucosa with ulcerative colitis and associated carcinomas or in the parenchymal cells of pancreas affected by pancreatitis, suggesting that chronic inflammation promotes impaired DNA repair function, thus increasing the risk for development of neoplasias in patients with these inflammatory diseases.^{6,7)} Although MSI is uncommon in ordinary lymphomas,⁸⁾ relatively frequent RER has been reported in gastric lymphoma of mucosa-associated lymphoid tissue type, which is known to develop from follicular gastritis caused by *Helicobacter pylori*^{9,10)} or AIDS-related lymphoma.¹¹⁾ These findings suggest that infection and chronic inflammation could be risk factors for neoplastic development through causing RER. As for PAL, biologically active metabolites including reactive oxygen species (ROS) produced in chronically inflamed pleural tissues could be causative in the development of lymphoma by

inducing RER. Because tumor cells in PAL contain Epstein-Barr virus (EBV) DNA,¹²⁾ EBV latent infection might enhance the genetic instability.¹³⁾

We previously established two B-cell lines from the biopsy specimens of two PAL patients: they had very complex karyotypes,¹⁴⁾ suggesting increased genome instability in these lines. In this study, four new lymphoma cell lines recently established from four cases with PAL were characterized in detail.

Materials and Methods

Patients. Four cell lines (OPL- 3, -4, -5, and -7) were established from biopsy specimens and peripheral blood samples of four patients (case 1, 2, 3, 4) after informed consent had been obtained. The clinicopathologic findings in these 4 patients, together with characteristics of the 4 cell lines, are summarized in Table 1. The patients suffered from chronic pyothorax resulting from artificial pneumothorax for the treatment of pulmonary tuberculosis. From 51 to 66 years after the onset of pyothorax, tumors developed in the pleural cavity. Biopsy samples were obtained. The histologic specimens were fixed in 10% formalin and routinely processed for paraffin-embedding. Histologic sections cut at 4 μ m were stained with hematoxylin and eosin and immunoperoxidase procedures. Histopathologic examination and immunophenotypic analyses of biopsy materials revealed diffuse large B-cell lymphoma in all cases. Cases 1, 3, and 4 were alive more than 1 year after biopsy, whereas case 2 died 1 year after the biopsy.

Cell cultures. Small pieces of the biopsy specimens obtained from the PAL lesions were washed several times with RPMI 1640 medium (Sigma, St. Louis, MO). Subsequently, culture (5×10^6 cells/ml) was started in RPMI 1640 supplemented with 20% heat-inactivated FCS at 37°C in 5% CO₂ in air. Heterologous feeder layers were not used for cell line establishment. EBV-positive (Raji) and -negative (Ramos) Burkitt's lymphoma cell lines obtained from the Japanese Cancer Research Resources Bank were also cultured and used for the experiment.

Immunohistochemistry and *in situ* hybridization. Immunophenotyping of the proliferating cells for B-, T-, NK-cell differentiation antigens and EBV antigens was performed on paraffin sections of the original tumor specimens using avidin-biotin-peroxidase complex method. The antibodies used were anti-CD20 (Kyowa Medex, Tokyo), CD79a, CD3 epsilon, CD45RO (UCHL-1), latent membrane protein (LMP) 1 (CS1-4), EB nuclear antigen (EBNA) 2 (PE2) (Dakopatts, Glostrup, Denmark), CD43 (MT-1) (Bioscience, Emmenbrucke, Switzerland), and CD56 (Novocastra, Newcastle, UK).

⁴To whom correspondence and reprint requests should be addressed. E-mail: aozasa@molpath.med.osaka-u.ac.jp

Table 1. Brief clinical findings of four cases and biological characteristics of the cell lines established from these cases

	Case 1 (OPL-3)	Case 2 (OPL-4)	Case 3 (OPL-5)	Case 4 (OPL-7)
Clinico-pathological features				
Age (yrs)	72	82	74	74
Sex	M	F	F	F
Duration of pyothorax (yrs)	51	63	66	54
Artificial pneumothorax	done	done	done	done
Histologic diagnosis	DLB	DLB	DLB	DLB
Initial treatment	CHOP	CHOP	CHOP	CHOP
Follow-up period	2 yrs	2 yrs	2 yrs	1 yr
Prognosis	CR	died	CR	CR
Microsatellite alterations	4/5 loci	0/5 loci	0/2 loci ¹⁾	0/2 loci ¹⁾
Growth characteristics				
Doubling time (hrs)	72	168	48	108
Saturation density (cells/ml)	2×10 ⁶	3×10 ⁵	5×10 ⁶	2×10 ⁶
Colony formation on soft agar	(+)	(-)	(+)	(-)
Surface phenotype	B cell type	B cell type	B cell type	B cell type
EBV status	monoclonal	monoclonal	monoclonal	monoclonal
Chromosome number	43-49	54-55	40-42	47
Presence of chromosomal abnormality	yes	yes	Yes	yes

1) Bat-25, Bat-26 locus were examined. DLB, diffuse large B-cell lymphoma; CR, complete remission. CHOP: cyclophosphamide, doxorubicin, vincristine, prednisolone.

RNA *in situ* hybridization using EBER1 probe was performed as previously described with some modification.¹⁵⁾ Briefly, 30-base oligonucleotide probes which were sense and anti-sense for a portion of the *EBER1* gene, a region of the EBV genome that is actively transcribed in latently infected cells, were synthesized using a DNA synthesizer. As the positive control, the Raji cell line was used. As negative controls, the hybridizing mixture containing sense probe or anti-sense probe after RNase treatment was used.

Flow cytometric analysis. OPL-3,-4,-5, and -7 were analyzed by 2 color immunofluorescence with a flow cytometer (EPICS XL, Beckman Coulter, Hialeah, FL). Antibodies conjugated with fluorescein isothiocyanate (FITC) or phycoerythrin (PE) (Becton Dickinson, Franklin Lakes, NJ) were used: they included anti-CD2, CD3, CD4, CD5, CD7, CD8, CD10, CD11c, CD15, CD16, CD19, CD20, CD21, CD23, CD24, CD25, CD30, CD34, CD38, CD56, CD103, surface IgM, surface IgD, surface IgG kappa chain, surface IgG lambda chain, cytoplasmic IgG kappa chain, cytoplasmic IgG lambda chain, and HLA-DR.

Immunoglobulin heavy chain and T-cell receptor gene rearrangement analysis. Rearrangement of the immunoglobulin heavy chain, and T-cell receptor *CB1* and *JB1* genes was analyzed by Southern blotting. Ten micrograms of DNA was digested with appropriate restriction enzyme, electrophoresed in 0.7% agarose gels, and Southern blotted. The filters were hybridized with J_H probe, CTβ and Jβ1 probe, respectively. Hybridizations were visualized by a Fluorescein Gene Image System (Amersham, Buckinghamshire, UK) according to the manufacturer's instructions.

Assessment of clonality of EBV. Ten micrograms of DNA extracted from cell lines was digested with *Bam*HI, then electrophoresed in 0.7% agarose gels and transferred to a nylon membrane. The filters were hybridized with *Bam*HI-NJhet fused terminal fragment of EBV to check the clonality of EBV genome. Since the fusion pattern of terminal repeats varies among EBV clones, the presence of a single dominant band of *Bam*HI-NJhet fragment represents clonal proliferation of EBV-infected cells.

Cytogenetic analysis. Chromosome analysis was performed in samples obtained from the cell lines by the trypsin-Giemsa banding method. Well-spread metaphases were photographed

and arranged according to the recommendations of ISCN (1995) for cancer cytogenetics.

Microsatellite analysis and mutation analysis of MSI target genes. According to the International Workshop on Microsatellite Instability and RER phenotypes in Cancer Detection and Familial Predisposition,¹⁶⁾ five microsatellite repeats, D2S123, D5S346, D17S250, BAT25, and BAT26 were analyzed in OPL-3 and -4, and two loci, BAT25 and BAT26 in OPL-5 and -7. After amplification, reaction products (3 μl) were denatured and separated on 6% polyacrylamide gels containing 7 M urea. The electrophoretic patterns of peripheral blood leukocytes, tumor tissues and cell lines from the same patient were then compared in order to detect different alleles, related to expansion or deletion of repeat tracts. The presence of frameshift mutations in the microsatellites in the coding regions of the following 6 genes were examined; *TGFβRII*, *IGF1IR*, *hMSH3*, *hMSH6*, *BAX*, and *E2F4*. Primers for PCR encompassing the stretch of mononucleotide or trinucleotide repeats in each gene are shown in Table 2.

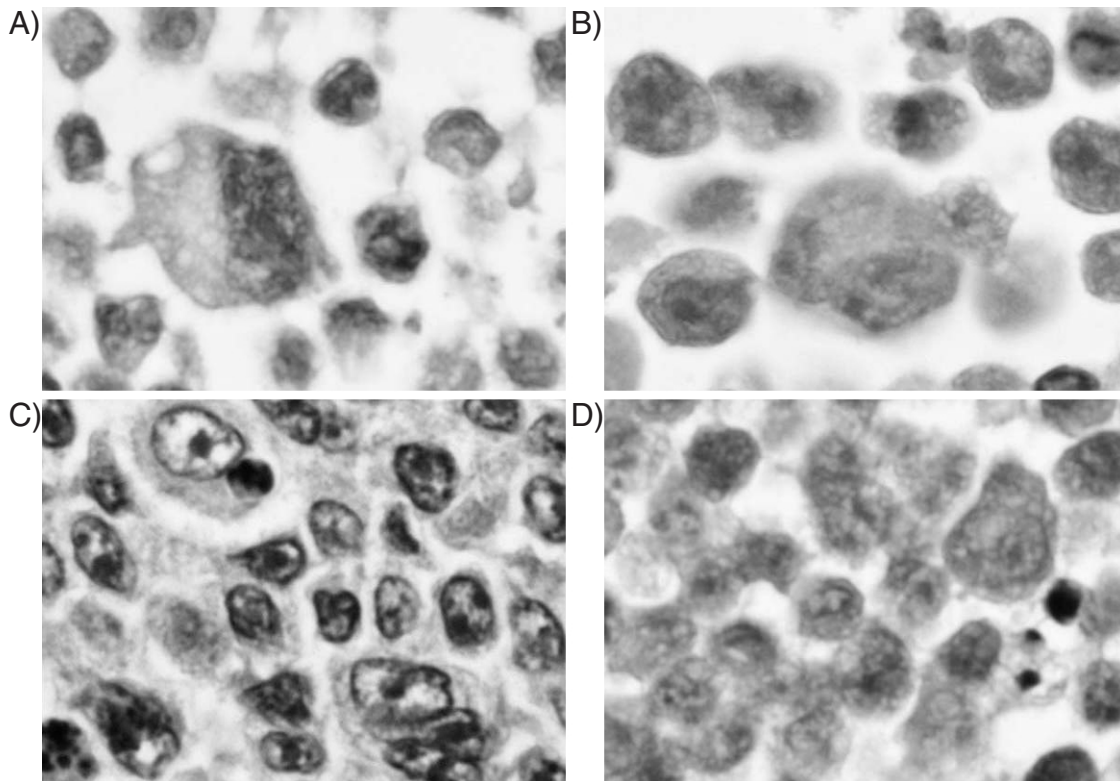
Results

Histologic findings of biopsy specimens. The tumors in all patients shared common histologic features, i.e., there was a monomorphic proliferation of predominantly large lymphoid cells. Immunohistochemical study (ABC method) of the paraffin sections revealed that the tumor cells in all cases were weakly positive for CD20, but negative for CD79a, CD45RO (UCHL-1), CD43 (MT-1), CD3 epsilon and CD56. *In situ* hybridization using EBER1 probe revealed positive signals in the nucleus of tumor cells in all cases. Tumor cells were positive for LMP1 in all cases and positive for EBNA2 in cases 1, 3, and 4.

Morphology and surface phenotype of established cell lines. All cell lines showed aggregation of large round cells with relative uniform size in OPL-7, whereas bizarre cells were occasionally seen in OPL-3, -4, and -5 (Fig. 1). Immunophenotypes of the cell lines are summarized in Table 3. OPL-3 expressed both CD2 and CD20, but did not express representative B-cell markers CD10, CD19, CD22, CD23, and CD24 or T-cell markers CD3, CD4, CD5, CD7, and CD8. OPL-4 also did not express representative B-cell markers except for CD20. OPL-5 ex-

Table 2. Oligonucleotide primers used for PCR reactions

	Primer sequence	PCR products (bp)
<i>D2S123</i>	5'-AAACAGGATGCCTGCCTTA-3' 5'-GGACTTTCCACCTATGGGAC-3'	197-227 (CA) <i>n</i>
<i>D5S346</i>	5'-ACTCACTCTAGTGATAAATCG-3' 5'-AGCAGATAAGACAGTATTACTAGTT-3'	96-122 (CA) <i>n</i>
<i>D17S250</i>	5'-GGAAGAATCAAATAGACAAT-3' 5'-GCTGGCCATATATATATTTAAACC-3'	150 (CA) <i>n</i>
<i>Bat-25</i>	5'-TCGCCTCCAAGAATGTAAGT-3' 5'-TCTGCATTTTAACTATGGCTC-3'	125 (A) 25
<i>Bat-26</i>	5'-TGACTACTTTTGACTTCAGCC-3' 5'-AACCATTC AACATTTTAAACC-3'	121 (A) 26
<i>hMSH3</i>	5'-GAGATAATGACTGATACTTCTACC-3' 5'-CATTTGTTCTCACCTGCAAAG-3'	131 (A) 8
<i>hMSH6</i>	5'-GGGTGATGGTCTATGTGTC-3' 5'-CGTAATGCAAGGATGGCGT-3'	93 (C) 8
<i>TGFβRII</i>	5'-CACTAGAGACAGTTTGCCATG-3' 5'-GCACTCATCAGAGCTACAGG-3'	142 (A) 10
<i>Bax</i>	5'-ATCCAGGATCGAGCAGGGCG-3' 5'-ACTCGCTCAGCTTCTTGGTG-3'	94 (G) 8
<i>IGFIIR</i>	5'-GCAGGTCTCTGACTCAGAA-3' 5'-GAAGAAGATGGCTGTGGAGC-3'	110 (G) 8
<i>E2F4</i>	5'-TGATAGCAAGGACAGTGGTGAG-3' 5'-AAAGGAGGTAGAAGGGTTGGGT-3'	177 (CAG) 13

**Fig. 1.** Morphology of established cell lines, OPL-3 (A), OPL-4 (B), OPL-5 (C), and OPL-7 (D).

pressed both CD15 and CD 20, but did not express representative B-cell markers CD10 and CD23, or T-cell markers CD3, CD4, CD5, CD7, and CD8. Dual-fluorescence analysis demonstrated the coexpression of CD2 and CD20 in OPL-3, and CD15 and CD20 in OPL-5 (Fig. 2). Three out of 4 cell lines expressed CD30, which is usually observed in EBV-positive cell lines, but did not express CD21, a receptor for EBV infection.

OPL-7 expressed surface Ig, and also representative B-cell markers, CD19, CD20, and CD23, without expressing T-cell markers, CD3, CD4, CD5, CD7, and CD8, indicating a relatively mature B-cell phenotype. Other lines did not express surface Ig at all.

Immunoglobulin heavy chain and T cell receptor gene rearrangement analysis. Southern blotting with use of J_H DNA probe dem-

Table 3. Phenotypic features of cell lines

	OPL-3	OPL-4	OPL-5	OPL-7
Flow cytometry	(%)	(%)	(%)	(%)
CD2	99.4	0.3	0.5	0.0
CD3	0.1	0.4	0.6	0.0
CD4	0.1	0.0	0	0.0
CD5	0.0	0.0	0	0.0
CD7	0.3	0.3	6.5	2.6
CD8	0.2	0.3	0.7	0.0
CD10	0.0	0.0	0.0	0.7
CD11c	8.1	9.1	ND	0.9
CD15	33.3	0.2	99.3	1.5
CD16	0.3	73.4	0.1	0.2
CD19	0.5	0.0	29.3	41.6
CD20	54.0	71.4	48.5	84.6
CD21	0.1	0.0	0.0	0.0
CD23	15.7	7.3	1.5	92.8
CD24	0.1	10.5	ND	ND
CD25	0.4	0.0	1.4	0
CD30	99.9	39.2	8.5	93.7
CD33	ND	ND	1.1	0
CD34	3.7	9.8	ND	ND
CD38	0.4	0.0	ND	ND
CD56	0.0	0.0	0.1	0.2
CD103	0.3	41.9	2.9	0.2
Surface IgM	0.0	0.0	0	0
Surface IgD	0.5	25.4	0.9	0.8
Surface IgG kappa	1.5	0.3	1.3	99.7
Surface IgG lambda	1.8	0.3	1.4	0.9
Cytoplasmic Ig kappa	0.1	1.5	ND	ND
Cytoplasmic Ig lambda	0.1	1.2	ND	ND
HLA-DR	0.6	18.8	ND	99.9
Immunohistochemistry				
LMP1	+		+	
EBNA2	+			+
EBERs ISH	+	+	+	+

onstrated the bands of monoclonal rearrangement of the *IgH* gene (Fig. 3). Monoclonal rearrangement was not found in T cell receptor gene (data not shown).

EBV association. Southern blot analysis for determination of the fusion pattern of EBV terminal repeats showed a single band in each cell line (Fig. 4). *In situ* hybridization using EBV1 probe revealed positive signals in the nuclei of many cells in all cell lines. The patterns of EBV latent gene expression were different. OPL-3 expressed LMP1 and EBNA2, OPL-5 expressed LMP1 but not EBNA2, OPL-7 expressed EBNA2 but not LMP1, and OPL-4 did not express either (Table 4).

Cytogenetic analysis. All cell lines showed highly complicated karyotypes, with numerous numerical and structural abnormalities. Although it is difficult to define a modal number of chromosomes in every cell line, common structural abnormalities were identified as follows: 43–49, XY, add (3)(q25), del (7)(q32), add (8)(p11), der (8), t(1;8)(q24;q24), del (12)(p11), add (13)(p11), add (17)(p11), add (18)(q21), –21, der (22), t(1;22)(q12;p11), del (1)(q21q25), +0–3 mar for OPL-3, 54–55, X, +add (1)(q11), der (1), add (1)(p36), add (1)(q21), +add (2)(p25), der (2), add (2)(p13), add (2)(q33), der (4), t(4;9)(p16;q11), +add (5)(q11), der (5), del (5)(p15), add (5)(q31), i (5)(q10), –6, add (6)(p21), +7, –9, del (9)(p21), add (10)(p11), add (11)(q23), add (11)(q23), add (12)(q24)x2, add (13)(q32), +14, –15, add (15)(p11), –16, add (16)(q22), –17, +20, mar1, mar2, mar3, mar4, mar5, +2–4 mar for OPL-4, 40–42, XX, –8, add (9)(p23), –10, der (12), del (p?) add (12)(q24), add (13)(p11), –15, add (15)(q22), –18, add (18)(q21), +add (19)(p13), add (19)(p13), –21, +mar1, +0–1

mar for OPL-5, 47, X, add (X)(q11), t(1;14)(q21;q22), t(2;13)(p10;p10), inv (5)(p15q33), –6, –7, add (8)(p21), add (9)(q34), der (10), t(6;10)(p11;p15), add (11)(p15), der (12), del (12)(p?), add (12)(q22), –13, add (19)(p11), add(19)(p13), der (19), t(7;19)(q11;p13), +mar1, +mar2x2 for OPL-7. There were no common abnormalities among the four cell lines.

Analysis of microsatellite instability and MSI target genes. Case 1 showed alterations at 4 of 5 loci examined, indicating that the tumors had RER phenotype (Fig. 5). Case 2 had no alterations at all. Then, the presence of frameshift mutations in microsatellites in the coding regions of 6 genes were examined (Fig. 5). Frameshift mutations in the *IGFIIR* and *hMSH6* genes were detected in OPL-3 and also in its parental tumor. Mutations in *E2F4* were detected in OPL-4, but not its parental tumor. No mutations were detected in OPL-5 and -7. These findings indicate that OPL-3, as well as its parental tumor, had RER phenotype.

Discussion

All four cell lines (OPL-3, -4, -5, and -7) were proved to be of B-cell origin through rearrangement analysis of Ig heavy chain gene and constant expression of CD20, but the expression patterns of surface antigens were unique and different from each other. Firstly, representative B-cell markers other than CD20 were frequently negative. Ordinary B-cell lymphoma cells rarely express CD2 and CD15, but OPL-3 and OPL-5 expressed CD2 and CD15, respectively. Recently Daibata *et al.*⁴⁾ reported that one PAL-derived cell line coexpressed CD2 and CD20 without expressing other representative B- and T-cell markers. Al Satti *et al.*³⁾ also reported the dual B- and T-cell antigen expression in PAL-derived cell line. PAL is unique not only in its clinical presentation, but also in its surface antigen expression.

All cell lines contained EBV DNA, with various expression patterns of EBV latent infection genes, *LMP1* and *EBNA2*. Two PAL cell lines previously reported by us also show different expression patterns.¹⁴⁾ In any case, PAL cells usually express LMP-1 and/or EBNA2. EBNA2 and LMP1 are essential for the transformation of B cells infected with EBV through activation of a variety of cellular genes, but these proteins serve as target molecules for the elimination of infected cells by cytotoxic T lymphocytes (CTLs).^{17, 18)} CD21, well-known EBV receptor on lymphocytes, were not expressed in any of the cell lines. EBV might possibly infect lymphocytes with CD21, but its expression might disappear after lymphomatous transformation.

Burkitt's lymphoma cells only express EBNA1, which is not recognized as a target by virus-specific CTLs, and thus can evade immune surveillance *in vivo*. Malignant lymphomas developing in immunocompromised hosts usually express EBNA2 and LMP1, but could evade immune surveillance by CTLs.^{17, 18)} Although systemic immunosuppressive conditions have not been noted in PAL patients, PAL cells frequently express EBNA2 and LMP1²⁾ *in vivo*. Therefore some mechanism for PAL cells to escape from host immune surveillance must be present. Production of immunosuppressive cytokine IL-10 by PAL cells, decreased or lost expression of HLA class I molecules in PAL cells, or mutation of the CTL-epitope in EBNA3B might work as mechanisms for escape of PAL cells from CTL.^{19, 20)}

Cell lines established from PAL, including the present ones, showed very complex karyotypes. Two PAL cell lines (OPL-1, -2) reported previously by us¹⁴⁾ also showed complex karyotypes with many numerical and chromosomal abnormalities. Lymphoma cell lines with EBV latent infection, such as those derived from Burkitt and NK/T cell lymphomas, also have chromosomal abnormalities, but not so complicated as those observed in PAL cell lines. Therefore, it is reasonable to con-

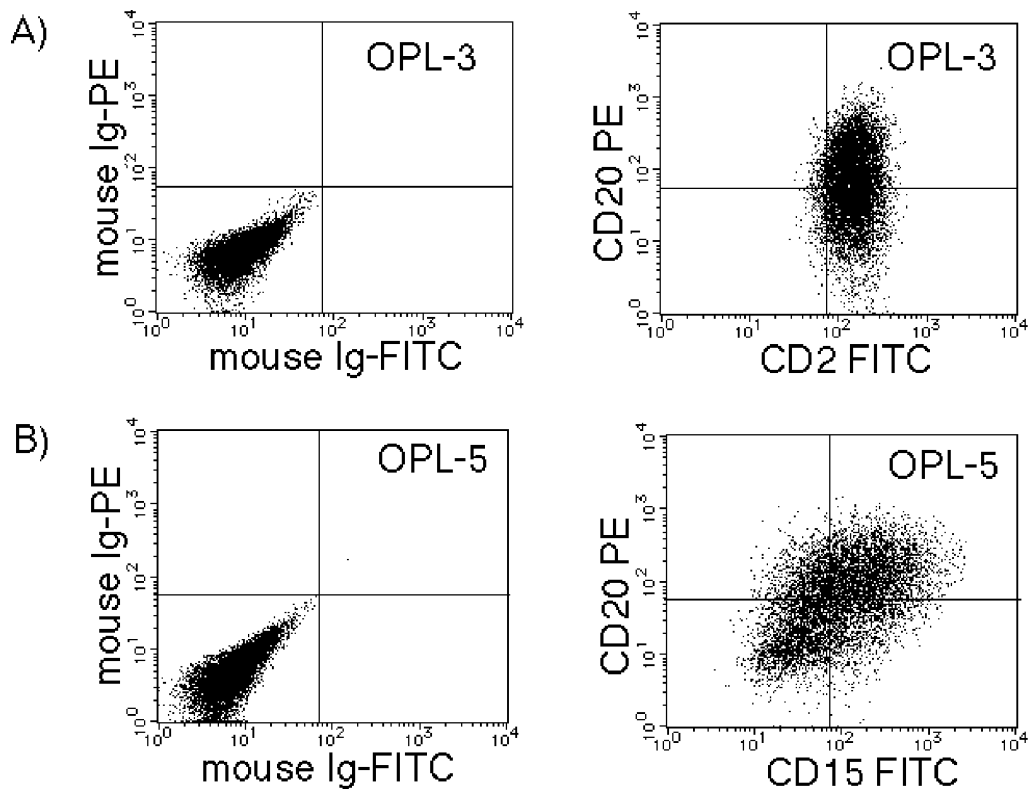


Fig. 2. Flow cytometric analysis of OPL-3 and OPL5 cells. Dual-fluorescence analysis showed coexpression of CD2 and CD20 antigens in OPL-3 (A), and coexpression of CD15 and CD20 in OPL-5 (B).

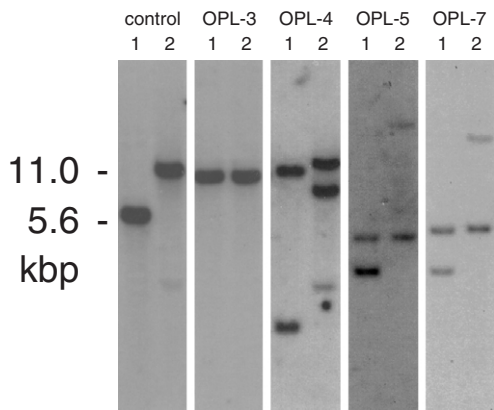


Fig. 3. Southern blot analysis of IgH rearrangement. Ten micrograms of DNA was digested with *Bam*HI (lane 1) and *Bam*HI+*Hind*III (lane 2), electrophoresed in 0.7% agarose gel, Southern blotted and hybridized with J_H DNA probe. Monoclonally rearranged bands were demonstrated in all four lines.

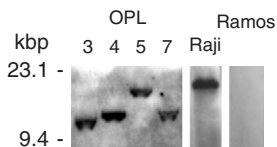


Fig. 4. Ten micrograms of DNA was digested with *Bam*HI, electrophoresed in 0.7% agarose gel, Southern blotted and hybridized with EBV *Bam*HI-NJhet DNA probe. A single band was found in all lines, indicating the presence of monoclonal EBV genome in these cell lines.

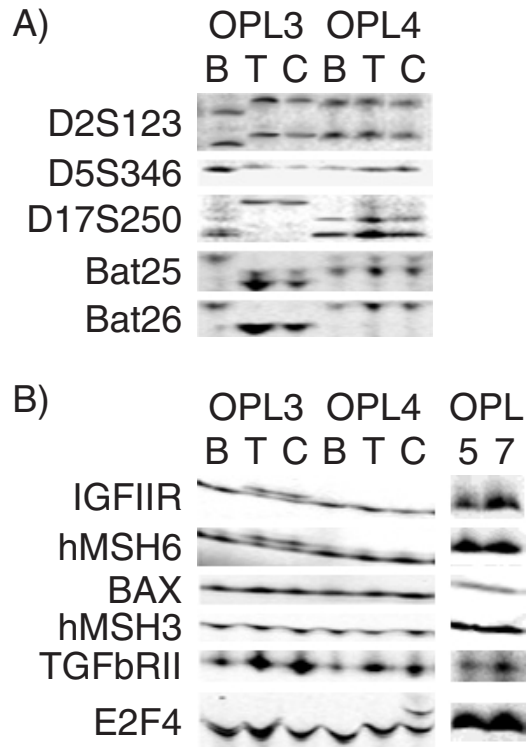


Fig. 5. PCR analyses of 5 microsatellite loci (A) and frameshift mutations within mono- and tri-nucleotide repeats of 6 genes, *TGF β RII*, *IGFIIR*, *hMSH3*, *hMSH6*, *BAX* and *E2F4*, in established cell lines (B). PCR products from established cell line (C), tumors (T) and corresponding peripheral blood leukocytes (B).

sider that highly complicated chromosomal abnormalities found in PAL could not be caused by EBV infection alone. Inflammatory products including reactive oxygen species produced in the chronically inflamed pleural tissues might be responsible for this phenomenon. Indeed, PAL develops in patients with more than 20 years' history of chronic pyothorax.^{1,2)} Defects of the genes maintaining genome stability might occur in the tumorigenesis of PAL.

MSH2, *PMS2*, and *MLH1* knockout mice are prone to develop lymphomas, suggesting that defects in mismatch repair (*MMR*) genes contribute to lymphomagenesis.^{21–23)} MSI is not a frequent phenomenon in nodal lymphoma.⁸⁾ However, MSI was reported to be rather frequent in extranodal lymphomas such as thyroid lymphoma²⁴⁾ and gastric lymphoma,^{9,10)} both of which diseases are known to develop in chronic inflammation. Therefore, it is possible that MSI is a frequent phenomenon in lymphomas developing in long-standing chronic inflammation.

Among lymphoid leukemia/lymphoma cell lines, 21% were reported to be MSI-positive.²⁵⁾ However, it is not clear whether target genes had already mutated *in vivo* or whether mutations occurred during *in vitro* cultures, because it was not stated whether the mutations were found in freshly prepared samples. Molenaar *et al.*²⁶⁾ reported that MSI and frameshift mutations in *BAX* and *TGFβRII* genes are uncommon in acute lymphoblastic leukemia *in vivo*, but frequent in cell lines. They concluded that *MMR* gene defects are uncommon in freshly isolated blasts, but

cells with defects in *MMR* gene were likely to be selected during the establishment of cell lines. In the present study, frameshift mutations in the *TGFβRII* and *hMSH6* genes were detected in OPL-3 and also in its parental tumor. These findings provide direct evidence that *MMR* defects may have been involved in lymphomagenesis in case 1. MSI was not present in the other three cell lines, suggesting that *MMR* genes were intact.

The characteristics of the four cell lines derived from PAL can be summarized as follows: B-cell nature with defective expression of B-cell and T-cell surface antigens, monoclonal pattern of EBV infection in lymphoma cells (indicating an etiological role of EBV in lymphomagenesis), complicated chromosomal abnormalities with numerous structural and numerical abnormalities, and occasional but distinct genome instability. These abnormalities in cell character might be caused by the specific circumstances of PAL lymphomagenesis, i.e., chronic inflammation. Thus, PAL cell lines could be useful for analysis of the molecular mechanisms through which malignancies develop in chronic inflammation.

We thank Drs. T. Osako (Kyoto City Hospital), Y. Tanio (Osaka Prefectural General Hospital), and N. Yonetani (Japanese Red Cross Society Wakayama Medical Center) for preparing the clinical materials and providing information. This work was supported by grants from the Ministry of Education, Culture, Sports, Science and Technology, Japan (14031213, 15026209, 15406013, 15590340).

- Nakatsuka S, Yao M, Hoshida Y, Yamamoto S, Iuchi K, Aozasa K. Pyothorax-associated lymphoma—a review of 106 cases. *J Clin Oncol* 2002; **20**: 4255–60.
- Iuchi K, Aozasa K, Yamamoto S, Mori T, Tajima K, Minato K, Mukai K, Komatsu H, Tagaki T, Kobashi Y, Yamabe H, Shimoyama M. Non-Hodgkin's lymphoma of the pleural cavity developing from long-standing pyothorax. Summary of clinical and pathological findings in thirty-seven cases. *Jpn J Clin Oncol* 1989; **19**: 249–57
- Al Satti T, Delecluze HJ, Chittal S, Brousset P, Magaud JP, Dastugue N, Cohen KE, Laurent G, Rubin B, Delsol G. A novel human lymphoma cell line (Deglis) with dual B/T phenotype and gene rearrangements and containing Epstein-Barr virus genomes. *Blood* 1992; **80**: 209–16.
- Daibata M, Taguchi T, Nemoto Y, Saito T, Machida H, Imai S, Miyoshi I, Taguchi H. Epstein-Barr virus (EBV)-positive pyothorax-associated lymphoma (PAL): chromosomal integration of EBV in a novel CD2-positive PAL B-cell line. *Br J Haematol*. 1994; **117**: 546–57
- Eshleman JR, Markowitz SD. Microsatellite instability in inherited and sporadic neoplasms. *Curr Opin Oncol* 1995; **7**: 83–9.
- Brentnall TA, Chen R, Lee JG, Kimmey MB, Bronner MP, Haggitt RC, Kowdley KV, Hecker LM, Byrd DR. Microsatellite instability and K-ras mutations associated with pancreatic adenocarcinoma and pancreatitis. *Cancer Res* 1995; **55**: 4264–7.
- Suzuki H, Harpaz N, Tarmin L, Yin J, Jiang HY, Bell JD, Hontanosas M, Groisman GM, Abraham JM, Meltzer SJ. Microsatellite instability in ulcerative colitis-associated colorectal dysplasias and cancers. *Cancer Res* 1994; **54**: 4841–4.
- Gamberi B, Gaidano G, Parsa N, Carbone A, Roncella S, Knowles DM, Louie DC, Shibata D, Chaganti RS, Dalla-Favera R. Microsatellite instability is rare in B-cell non-Hodgkin's lymphomas. *Blood* 1997; **89**: 975–9.
- Chong JM, Fukayama M, Hayashi Y, Hishima T, Funata N, Koike M, Matsuya S, Konishi M, Miyaki M. Microsatellite instability and loss of heterozygosity in gastric lymphoma. *Lab Invest* 1997; **77**: 639–45.
- Peng H, Chen G, Du M, Singh N, Isaacson PG, Pan L. Replication error phenotype and p53 gene mutation in lymphomas of mucosa-associated lymphoid tissue. *Am J Pathol* 1996; **148**: 643–8.
- Bedi GC, Westra WH, Farzadegan H, Pitha PM, Sidransky D. Microsatellite instability in primary neoplasms from HIV+ patients. *Nat Med* 1995; **1**: 65–8.
- Fukayama M, Ibuka T, Hayashi Y, Ooba T, Koike M, Mizutani S. Epstein-Barr virus in pyothorax-associated pleural lymphoma. *Am J Pathol* 1993; **143**: 1044–9.
- Gualandi G, Giselicio L, Carloni M, Palitti F, Mosesso P, Alfonsi AM. Enhancement of genetic instability in human B cells by Epstein-Barr virus latent infection. *Mutagenesis* 2001; **16**: 203–8.
- Kanno H, Yasunaga Y, Ohsawa M, Taniwaki M, Iuchi K, Naka N, Torikai K, Shimoyama M, Aozasa K. Expression of Epstein-Barr virus latent infection genes and oncogenes in lymphoma cell lines derived from pyothorax-associated lymphoma. *Int J Cancer* 1996; **67**: 86–94.
- Weiss LM, Jaffe ES, Liu XF, Chen YY, Shibata D, Medeiros LJ. Detection and localization of Epstein-Barr viral genomes in angioimmunoblastic lymphadenopathy and angioimmunoblastic lymphadenopathy-like lymphoma. *Blood* 1992; **79**: 1789–95.
- Boland CR, Thibodeau SN, Hamilton SR, Sidransky D, Eshleman JR, Burt RW, Meltzer SJ, Rodriguez BM, Fodde R, Ranzani GN, Srivastava S. A National Cancer Institute Workshop on Microsatellite Instability for cancer detection and familial predisposition: development of international criteria for the determination of microsatellite instability in colorectal cancer. *Cancer Res* 1998; **58**: 5248–57.
- Wolf H, Bogedain C, Schwarzmann F. Epstein-Barr virus and its interaction with the host. *Intervirology* 1993; **35**: 26–39.
- Rickinson AB, Murray RJ, Brooks J, Griffin H, Moss DJ, Masucci MG. T cell recognition of Epstein-Barr virus associated lymphomas. *Cancer Surv* 1992; **13**: 53–80.
- Kanno H, Naka N, Yasunaga Y, Aozasa K. Role of an immunosuppressive cytokine, interleukin-10, in the development of pyothorax-associated lymphoma. *Leukemia* 1997; **3**: 525–6.
- Kanno H, Nakatsuka S, Iuchi K, Aozasa K. Sequences of cytotoxic T-lymphocyte epitopes in the Epstein-Barr virus (EBV) nuclear antigen-3B gene in a Japanese population with or without EBV-positive lymphoid malignancies. *Int J Cancer* 2000; **88**: 626–32.
- Baker SM, Plug AW, Prolla TA, Bronner CE, Harris AC, Yao X, Christie DM, Monell C, Arnheim N, Bradley A, Ashley T, Liskay RM. Involvement of mouse Mlh1 in DNA mismatch repair and meiotic crossing over. *Nat Genet* 1996; **13**: 336–42.
- Lowsky R, DeCoteau JF, Reitmaier AH, Ichinohasama R, Dong WF, Xu Y, Mak TW, Kadin ME, Minden MD. Defects of the mismatch repair gene *MSH2* are implicated in the development of murine and human lymphoblastic lymphomas and are associated with the aberrant expression of thombotin-2 (*Lmo-2*) and *Tal-1* (*SCL*). *Blood* 1997; **89**: 2276–82.
- Prolla TA, Baker SM, Harris AC, Tsao JL, Yao X, Bronner CE, Zheng B, Gordon M, Reneker J, Arnheim N, Shibata D, Bradley A, Liskay RM. Tumour susceptibility and spontaneous mutation in mice deficient in *Mlh1*, *Pms1* and *Pms2* DNA mismatch repair. *Nat Genet* 1998; **18**: 276–9.
- Takakuwa T, Hongyo T, Syaifudin M, Kanno H, Matsuzuka F, Narabayashi I, Nomura T, Aozasa K. Microsatellite instability and *k-ras*, *p53* mutations in thyroid lymphoma. *Jpn J Cancer Res* 2000; **91**: 280–6.
- Kodera T, Kohno T, Takakura S, Morishita K, Hamaguchi H, Hayashi Y, Sasaki T, Yokota J. Microsatellite instability in lymphoid leukemia and lymphoma cell lines but not in myeloid leukemia cell lines. *Genes Chromosomes Cancer* 1999; **26**: 267–9.
- Molenaar JJ, Gerard B, Chambon PC, Cave H, Duval M, Vilmer E, Grandchamp B. Microsatellite instability and frameshift mutations in *BAX* and transforming growth factor-beta RII genes are very uncommon in acute lymphoblastic leukemia *in vivo* but not in cell lines. *Blood* 1998; **92**: 230–3.